APPLIED AND ENVIRONMENTAL MICROBIOLOGY, Oct. 1989, p. 2588–2591 Vol. 55, No. 10
0099-2240/89/102588-04$02.00/0
Copyright © 1989, American Society for Microbiology

Synergistic Competitive Inhibition of Ferrous Iron Oxidation by *Thiobacillus ferrooxidans* by Increasing Concentrations of Ferric Iron and Cells

HECTOR M. LIZAMA AND ISAMU SUZUKI*

Department of Microbiology, University of Manitoba, Winnipeg, Manitoba, Canada R3T 2N2

Received 18 May 1989/Accepted 17 July 1989

Oxidation of ferrous iron by *Thiobacillus ferrooxidans* SM-4 was inhibited competitively by increasing concentrations of ferric iron or cells. A kinetic analysis showed that binding of one inhibitor did not exclude binding of the other and led to synergistic inhibition by the two inhibitors. Binding of one inhibitor, however, was affected by the other inhibitor, and the apparent inhibition constant increased with increasing concentrations of the other inhibitor.

Thiobacillus ferrooxidans oxidizes ferrous iron to ferric iron with atmospheric oxygen: $4Fe^{2+} + O_2 + 4H^+ \rightarrow 4Fe^{3+} + 2H_2O$, an important reaction in the bacterial leaching of metals from sulfide ores (5, 10). The product of oxidation, Fe^{3+}, inhibits Fe^{2+} oxidation competitively (1). Our recent work has demonstrated that Fe^{2+} oxidation by some *T. ferrooxidans* strains is also competitively inhibited by increasing concentrations of cells (8).

We have now studied the effect of increasing cell concentrations on competitive inhibition of Fe^{2+} oxidation by Fe^{3+}. The results agree with the concept that both Fe^{3+} and cells compete with Fe^{2+} for the Fe^{2+}-binding site of Fe^{2+}-oxidizing cells, but binding of one inhibitor does not exclude binding of the other, although the apparent inhibition constant for the latter increases with increasing concentrations of the former.

MATERIALS AND METHODS

Microorganism. The *T. ferrooxidans* strain used in this study, SM-4, was isolated from a sulfide ore mine site (4) and grown in a medium with $FeSO_4 \cdot 7H_2O$ (33.3 g/liter) as described previously (4, 6).

Ferrous-iron-oxidizing activity. The rate of Fe^{2+} oxidation was determined by measuring the rate of O_2 consumption at 25°C in a Gilson oxygraph with a Clarke electrode. The reaction was performed in growth medium containing the following minus $FeSO_4 \cdot 7H_2O$: 0.4 g of $(NH_4)SO_4$, 0.1 g of K_2HPO_4, and 0.4 g of $MgSO_4$ per liter (adjusted to pH 2.3 with H_2SO_4). A total volume of 1.2 ml contained microliter volumes of a cell suspension (50 mg of wet cells per ml), 50 mM $Fe_2(SO_4)_3$, and 0.1 M $FeSO_4 \cdot 7H_2O$ at pH 2.3. The reaction was started by addition of Fe^{2+} as the substrate, and the initial linear rate of O_2 consumption (nanomoles of O_2 per minute) was taken as the reaction rate. The reaction rate was plotted against the concentration of Fe^{2+} in double-reciprocal Lineweaver-Burk plots (3).

RESULTS

Oxidation of Fe^{2+} by *T. ferrooxidans* SM-4 cells was competitively inhibited by Fe^{3+} at three fixed concentrations of cells (0.25 [A]; 0.50 [B], and 1.00 [C] mg of cells) as shown in the double-reciprocal reaction rate -Fe^{2+} concentration plots of Fig. 1. The replot of the slope against the Fe^{3+} concentration (Fig. 2) indicated that increasing cell concentrations lowered both the slopes and y intercepts but increased the values of apparent inhibition constants for Fe^{3+} (the positive value of x intercepts). The secondary replot of the slope change from Fig. 2 showed that the slope increased with the reciprocal of the cell concentrations (Fig. 2, inset).

When the data were plotted at fixed Fe^{3+} concentrations (0 [A], 2 [B], 8 [C], and 16 [D] mM Fe^{3+}), the patterns in Fig. 3 were obtained in which increasing cell concentrations lowered both the y intercepts and slopes and characteristically increased the apparent K_m values (the positive value of the reciprocal of the x intercepts), similarly to our previous results (8).

When the reaction rate, v (nanomoles of O_2 per minute), was converted to the specific activity or rate v_{sp} (v divided by the concentration of cells), and plotted in a double-reciprocal manner against the Fe^{2+} concentration (8), the resulting plots (Fig. 4) showed competitive inhibition by increasing concentrations of cells at four fixed Fe^{3+} concentrations of 0 to 16 mM (A to D). The replot of the slope against the cell concentrations (Fig. 5) indicated an increase in the apparent inhibition constants for cells in Fe^{3+} and stronger inhibition by cells at higher Fe^{3+} concentrations (Fig. 5, insets).

These results can be explained if Fe^{3+} and cells both compete with Fe^{2+} for the Fe^{2+} oxidation sites of cells and binding of one inhibitor (Fe^{3+} or cells) does not exclude binding of the other (cells or Fe^{3+}) but only inhibits it. Segel (7) discussed the inhibition of an enzyme (E) by two competitive inhibitors (I and X) with respect to the substrate (S) in the formation of a product (P):

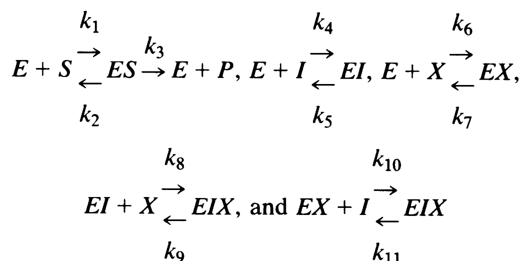

$$E + S \underset{k_2}{\overset{k_1}{\rightleftarrows}} ES \xrightarrow{k_3} E + P,\ E + I \underset{k_5}{\overset{k_4}{\rightleftarrows}} EI,\ E + X \underset{k_7}{\overset{k_6}{\rightleftarrows}} EX,$$

$$EI + X \underset{k_9}{\overset{k_8}{\rightleftarrows}} EIX, \text{ and } EX + I \underset{k_{11}}{\overset{k_{10}}{\rightleftarrows}} EIX$$

The formation of EIX distinguishes this synergistic system from inhibition by mutually exclusive inhibitors.

The rate equation derived by Segel (7) is rearranged as:

* Corresponding author.

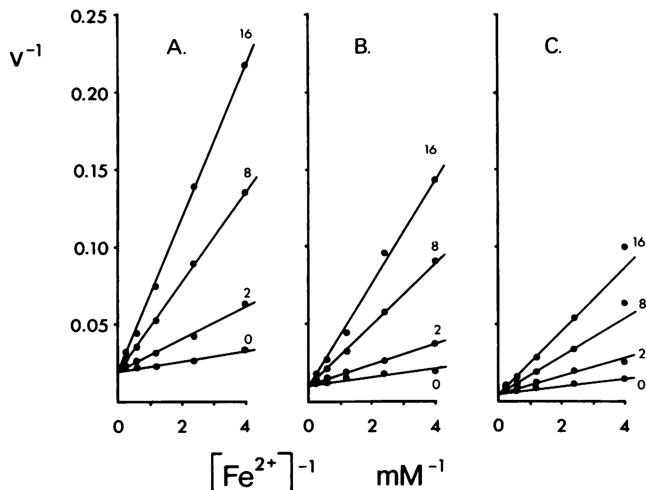

FIG. 1. Competitive inhibition of Fe^{2+}-oxidizing activity of cells by increasing concentrations of Fe^{3+} at fixed concentrations of cells. The O_2 consumption rate (v) was determined as nanomoles of O_2 per minute at 25°C, as described in Materials and Methods, at various Fe^{2+} concentrations. The concentrations of Fe^{3+} were 0, 2, 8, and 16 mM, as shown. The amounts of cells used were 0.25, 0.50, and 1.00 mg of wet cells in a total volume of 1.2 ml in A, B, and C, respectively.

$$v = \frac{k_3[E][S]}{[S] + K_s\{1 + [I]/K_i + [X]/K_x + ([I][X]/(\alpha K_i K_x)\}} \quad (1)$$

where v is the reaction rate; $[E]$, $[S]$, $[I]$, and $[X]$ are concentrations of E, S, I and X; and K_i and K_x are inhibition constants for I and X, k_5/k_4, and k_7/k_6, respectively. K_s is the dissociation constant for S, k_2/k_1, and is the same as the Michaelis constant when $k_2 \gg k_3$. When binding of one inhibitor does not affect binding of the other, $\alpha = 1$, $K_i = k_5/k_4 = k_{11}/k_{10}$, and $K_x = k_7/k_6 = k_9/k_8$.

We have previously derived a rate equation for competitive inhibition of *T. ferrooxidans* Fe^{2+} oxidation by increasing *T. ferrooxidans* cell concentrations (8):

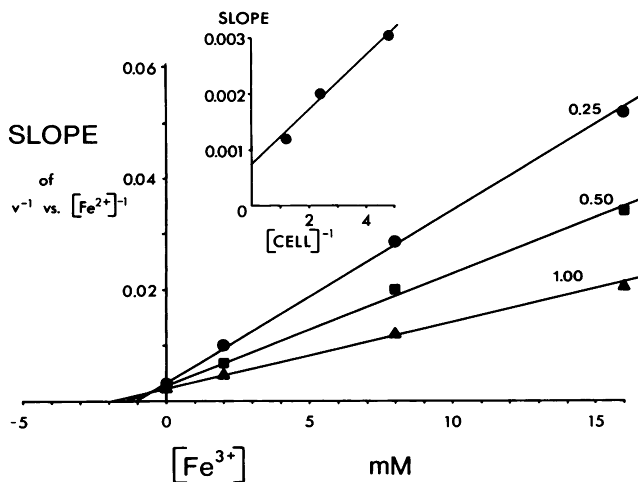

FIG. 2. Replot of the slope from Fig. 1 against the concentration of Fe^{3+}. The amounts of cells used for the lines were 0.25, 0.50, and 1.00 mg of wet cells in 1.2 ml, as indicated. The inset is the secondary replot of the slope against the reciprocal of the cell concentration (milligrams of wet cells per milliliter).

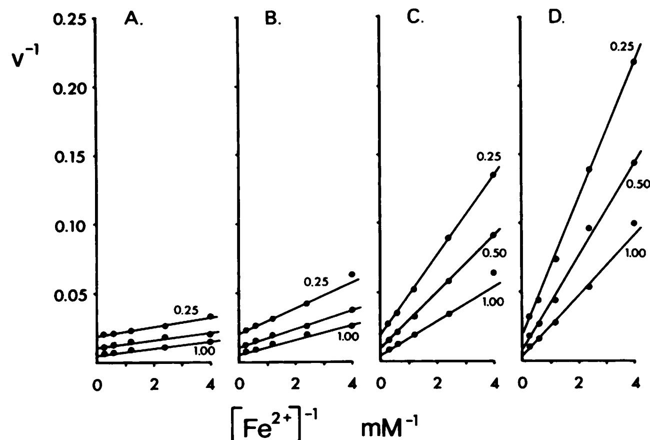

FIG. 3. Effect of Fe^{2+} concentration on the Fe^{2+}-oxidizing activity of various concentrations of cells at fixed concentrations of Fe^{3+}. The data were the same as in Fig. 1. Three lines in each graph represent the data at 0.25, 0.50, and 1.00 mg of wet cells in a total volume of 1.2 ml. Four graphs (A through D, respectively) represent the data obtained with 0, 2, 8, and 16 mM Fe^{3+}.

$$v = \frac{k_3'[C][Fe^{2+}]}{[Fe^{2+}] + K_m(1 + [C]/K_i')} \quad (2)$$

where $[C]$ is the concentration of cells, k_3' is k_3 times the number of enzyme per cell, $[Fe^{2+}]$ is the concentration of Fe^{2+}, and K_i' is K_i divided by the number of inhibitor per cell.

With Fe^{3+} as the second competitive inhibitor, the rate equation becomes:

$$v = \frac{k_3'[C][Fe^{2+}]}{[Fe^{2+}] + K_m\{1 + [C]/K_i' + [Fe^{3+}]/K_{if} + ([C][Fe^{3+}])/(\alpha\, k_i'K_{if})\}} \quad (3)$$

where K_{if} is the inhibition constant for Fe^{3+} and $[Fe^{3+}]$ is the concentration of Fe^{3+}.

In double-reciprocal form, the equation becomes:

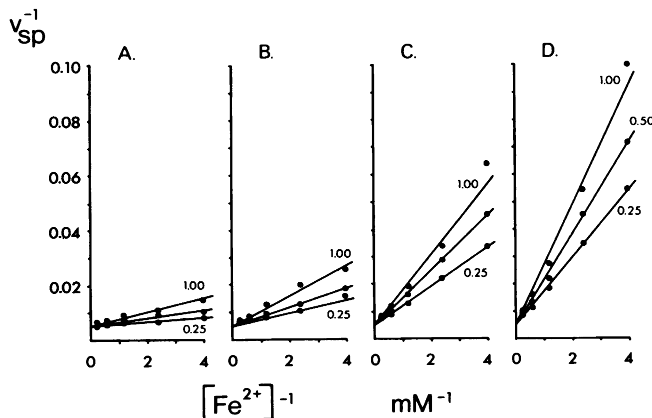

FIG. 4. Competitive inhibition of Fe^{2+}-oxidizing activity of cells by increasing concentrations of cells. The specific activity or rate (v_{sp}) was calculated on the basis of the data in Fig. 3 as nanomoles of O_2 per minute per milligram of wet cells per milliliter. The other conditions were as described in the legend to Fig. 3.

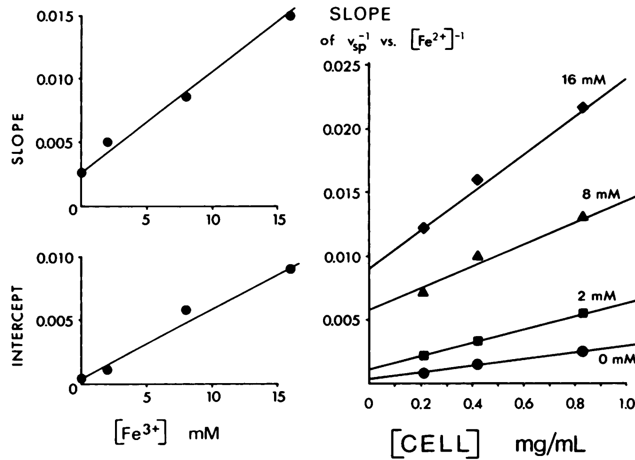

FIG. 5. Replot of slopes from Fig. 4 against the concentration of cells. The concentrations of Fe^{3+} used for the lines were 0, 2, 8, and 16 mM, as shown. The inset is the secondary replot of the slope and intercept against the concentration of Fe^{3+}.

$$1/v = 1/k_3'[C] + K_m/k_3'[C]\ \{1 + [C]/K_i' + [Fe^{3+}]/K_{if} + ([C][Fe^{3+}])/(\alpha K_i' K_{if})\}(1/[Fe^{2+}]) \quad (4)$$

Thus, plots of $1/v$ versus $1/[Fe^{2+}]$ at a fixed $[C]$ and different values of $[Fe^{3+}]$ should intersect on the y axis at $1/(k_3'\ [C])$ with slopes increasing with $[Fe^{3+}]$, which is typical of competitive inhibition patterns (Fig. 1). The slope replots against $[Fe^{3+}]$ (Fig. 2) should intersect the y axis at $\{K_m/(k_3[C]) + K_m/(k_3'\ K_i')\}$ and the x axis at $-K_{if}(1 + [C]/K_i')/\{1 + [C]/(\alpha K_i')\}$ and have slopes equal to $\{K_m/(k_3'\ [C]K_{if}) + K_m/(k_3'\alpha K_i'\ K_{if})\}$. The secondary replot of the slopes against $1/[C]$ (Fig. 2, inset) should have a slope of $K_m/(k_3'\ K_{if})$ and an intercept on the y axis at $K_m/(k_3'\alpha K_i'\ K_{if})$ and on the x axis at $-1/(\alpha K_i')$.

The plots at a fixed $[Fe^{3+}]$ and various values of $[C]$ (Fig. 3) produced patterns different from Fig. 1, and the y intercept and slope both decreased with increasing $[C]$ because of the $1/[C]$ term in equation 4. In our previous paper (8), we used the specific activity or rate, v_{sp}, by dividing v by the cell concentration, $[C]$, to demonstrate competitive inhibition. Equation 4 becomes:

$$1/v_{sp} = 1/k_3 + K_m/k_3\{1 + [C]/K_i' + [Fe^{3+}]/K_{if} + ([C][Fe^{3+}])/(\alpha K_i' K_{if})\}(1/[Fe^{2+}]) \quad (5)$$

Now the double-reciprocal plots of v_{sp} versus $[Fe^{2+}]$ at a fixed $[Fe^{3+}]$ should show a typical competitive inhibition pattern by $[C]$ (Fig. 4) with lines intersecting the y axis at $(1/k_3')$. The slope replot against $[C]$ (Fig. 5) should show a family of lines at different values of $[Fe^{3+}]$ with y intercepts of $\{K_m/k_3' + (K_m[Fe^{3+}])/(k_3'\ K_{if})\}$ and x intercepts of $-K_i'\ (1 + [Fe^{3+}]/K_{if})/\{1 + [Fe^{3+}]/(\alpha K_{if})\}$ and slopes of $\{K_m/(k_3'\ K_i') + (K_m[Fe^{3+}])/(k_3'\alpha K_i'\ K_{if})\}$. The secondary replot of slopes against $[Fe^{3+}]$ (Fig. 5, inset) should intersect the y axis at $\{K_m/(k_3'\ K_i')\}$ and the x axis at $(-\alpha K_{if})$. The secondary replot of y intercepts (Fig. 5, inset) should intersect the y axis at (K_m/k_3') and the x axis at $(-K_{if})$.

The rate and kinetic constants obtained from the results are shown in Table 1. An α value larger than 1 indicates that binding of one inhibitor decreases the binding constant of the other inhibitor (7), i.e., increases the apparent inhibition constant. This is evident in Fig. 2 and 5, in which the apparent K_{if} and K_i' (positive values of x intercepts) increased with increasing concentrations of the other inhibitor.

Fig. 6 and 7 are Dixon plots as described by Segel (7) drawn to confirm our interpretation of the results. The reciprocal of v_{sp} at an $[Fe^{2+}]$ of 0.42 mM was plotted against $[Fe^{3+}]$ at three different $[C]$ values (Fig. 6). The changing slope indicates that the two inhibitors are not exclusive of each other in the inhibition. The lines intersect at the negative x coordinate corresponding to αK_{if}, i.e., a 3.2 mM $[Fe^{3+}]$. Similar plots against $[C]$ at four different $[Fe^{3+}]$

TABLE 1. Rate and kinetic constants

Constant	Value
k_3'	200 nmol of O_2 per min per mg of wet cells
K_m	70 μM $[Fe^{2+}]$
K_i'	135 μg of wet cells per ml
K_{if}	640 μM $[Fe^{3+}]$
α	5

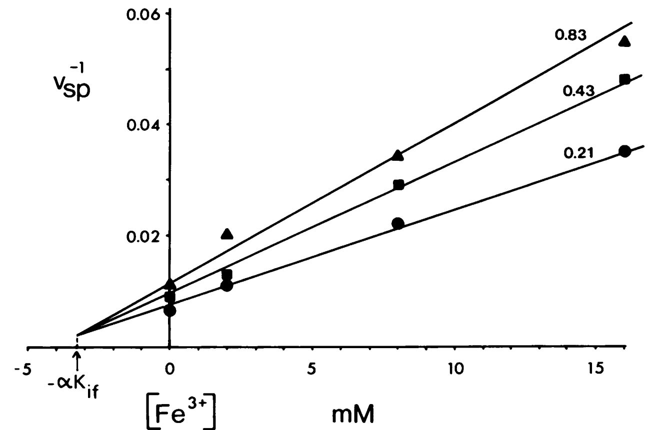

FIG. 6. Plot of the reciprocal of v_{sp} against the concentration of Fe^{3+}. The data were obtained from Fig. 4 at a fixed Fe^{2+} concentration of 0.42 mM. Each line represents values at a cell concentration of 0.21, 0.43, or 0.83 mg of wet cells per milliliter, as shown.

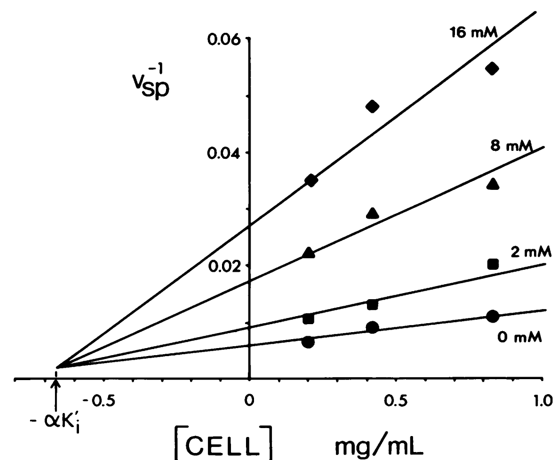

FIG. 7. The plot of the reciprocal of v_{sp} against the concentration of cells. The data were obtained from Fig. 4 at a fixed Fe^{2+} concentration of 0.42 mM. Each line represents values at an Fe^{3+} concentration of 0, 2, 8, or 16 mM, as shown.

values produced Fig. 7. Four lines of different slopes intersected at the negative x coordinate of $\alpha K_i'$, i.e., 0.66 mg of wet cells per ml. These values are very close to the values expected on the basis of those in Table 1.

When the specific activity or rate (v_{sp}) was used, inhibition by either Fe^{3+} or cells was greater when the other inhibitor concentration, $[C]$ or $[Fe^{3+}]$, was higher; i.e., there was a synergistic inhibition effect (Fig. 6 and 7).

DISCUSSION

There are complex interactions during Fe^{2+} oxidation by *T. ferrooxidans* among the cells as the Fe^{2+}-oxidizing catalyst, Fe^{2+} as the substrate, Fe^{3+} as the product of oxidation and a competitive inhibitor of Fe^{2+} oxidation, and also the cells as a competitive inhibitor of Fe^{2+} oxidation. These interactions should affect the rate of bacterial leaching of sulfide minerals in addition to other factors, such as the air supply, nutrients, temperature, pH, and toxic metals.

The results of this study indicate that, with *T. ferrooxidans* SM-4, both cells and Fe^{3+} act as competitive inhibitors of Fe^{2+} in its oxidation by cells and that inhibition is not mutually exclusive; i.e., both inhibitors can bind the Fe^{2+}-oxidizing system simultaneously, resulting in stronger inhibition than by each separately because of the formation of an additional inactive form (*EXI*). Binding of the second inhibitor, however, is inhibited by the first inhibitor, since α is larger than 1. Therefore, the apparent inhibition constants increase with the increasing concentration of the other inhibitor.

When *T. ferrooxidans* cells grow in a Fe^{2+}-containing medium, the rate of Fe^{2+} oxidation is initially governed by the Michaelis-Menten equation $v = k_3' [C]/([Fe^{2+}] + K_m)$, but when the concentrations of cells and Fe^{3+} increase, the apparent K_m values increase because of competitive inhibition by cells and Fe^{3+}. The high concentration of Fe^{2+} used in normal growth medium is essential to overcome this effect. Precipitation of insoluble Fe^{3+} (5, 10) reduces the concentration of Fe^{3+} and therefore its inhibitory effect.

The rate of Fe^{2+} oxidation in a culture growing in Fe^{2+} increases when the cell concentration increases, but the specific activity (Fe^{2+} oxidation rate per milligram of cells) decreases because of competitive inhibition by cells when the Fe^{2+} concentration is not saturating. In our culture of SM-4 in Fe^{2+}-containing medium, the cell concentration reached 20 to 50 μg of wet cells per ml, which is below the K_i value of 135 μg of wet cells per ml; therefore, the inhibition was not very significant. The inhibition becomes more significant in experiments in which concentrated cell suspensions are used at low Fe^{2+} concentrations, as in this work. Since only *T. ferrooxidans* strains recently isolated demonstrated this anomalous property (8), it is possibly related to their mode of growth on the surface of sulfide ores. We have studied the effect of cell concentration on pyrite oxidation, and the results will be reported later.

The K_m, K_i', and K_{if} values shown in Table 1 are minimum values and are considerably lower than those previously reported for apparent K_m values of 0.33 to 9.4 mM or higher $[Fe^{2+}]$ (1, 9), apparent K_{if} values of 1.2 to 28 mM $[Fe^{3+}]$ (1, 9), and a K_i' value for the SM-4 strain of 0.33 mg of wet cells per ml (8). The last value was perhaps higher because of the lower activity of the cells (k_3', 125 instead of 200 nmol of O_2 per min per mg of wet cells) or simply because different batches of cells were used. The relatively low K_{if} value raises the possibility that the observed inhibition by cells was caused by Fe^{3+} introduced with the cell suspension. The possibility of inhibition by free Fe^{3+} was eliminated by calculating the effect of low concentrations of Fe^{3+} found in the cell suspension. This does not exclude the possible cause of inhibition suggested in our previous paper (8), i.e., that the special Fe^{3+} coat on the surface of the cells makes contact with Fe^{2+}-oxidizing cells. Inhibition by Fe^{3+} formed from Fe^{2+} was also considered negligible, since the oxidation rate was determined as the initial linear reaction rate before accumulation of any significant concentration of Fe^{3+}.

It is interesting that Fe^{3+} inhibition of Fe^{2+} oxidation by *T. ferrooxidans* was found to be less pronounced at lower temperatures (2). The apparent K_{if} value dramatically increased (15-fold) when the temperature was lowered from 27 to 5°C. Perhaps secondary binding of inhibitors to form *EIX* is more difficult at lower temperatures (higher α values), although it is possible that K_{if} itself is affected by temperature.

ACKNOWLEDGMENTS

We thank the Natural Sciences and Engineering Research Council of Canada for grants to I.S. and a postgraduate fellowship to H.M.L. and CANMET (Canada Centre for Mineral & Energy Technology) for ongoing interest and support.

LITERATURE CITED

1. **Kelly, D. P., and C. A. Jones.** 1978. Factors affecting metabolism and ferrous iron oxidation in suspensions and batch cultures of *Thiobacillus ferrooxidans*: relevance to ferric iron leach solution regeneration, p. 19–44. *In* L. E. Murr, A. E. Torma, and J. A. Brierley (ed.), Metallurgical applications of bacterial leaching and related microbiological phenomena. Academic Press, Inc., New York.
2. **Kovalenko, T. V., G. I. Karavaiko, and V. P. Piskunov.** 1982. Effect of Fe^{3+} ions in the oxidation of ferrous iron by *Thiobacillus ferrooxidans* at various temperatures. Mikrobiologiya **51**:156–160.
3. **Lineweaver, H., and D. Burk.** 1934. The determination of enzyme dissociation constants. J. Am. Chem. Soc. **58**:658–666.
4. **Lizama, H. M., and I. Suzuki.** 1988. Bacterial leaching of a sulfide ore by *Thiobacillus ferrooxidans* and *Thiobacillus thiooxidans*. 1. Shake flask studies. Biotechnol. Bioeng. **32**: 110–116.
5. **Lundgren, D. G., and M. Silver.** 1980. Ore leaching by bacteria. Annu. Rev. Microbiol. **34**:263–283.
6. **McCready, R. G. L., D. Wadden, and A. Merchbank.** 1986. Nutrient requirements for the in-place leaching of uranium by *Thiobacillus ferrooxidans*. Hydrometallurgy **17**:61–71.
7. **Segel, I. H.** 1975. System B3. Cooperative (synergistic) pure competitive inhibition by two different nonexclusive inhibitors, p. 481–488. *In* Enzyme kinetics. John Wiley & Sons, Inc., New York.
8. **Suzuki, I., H. M. Lizama, and P. D. Tackaberry.** 1989. Competitive inhibition of ferrous iron oxidation by *Thiobacillus ferrooxidans* by increasing concentrations of cells. Appl. Environ. Microbiol. **55**:1117–1121.
9. **Suzuki, I., J. K. Oh, P. D. Tackaberry, and H. Lizama.** 1988. Determination of activity parameters in *Thiobacillus ferrooxidans* strains as criteria for mineral leaching efficiency. I. Growth characteristics and effect of metals on growth and on sulfur or ferrous iron oxidation, p. 179–209. *In* R. G. L. McCready (ed.), Biominet proceedings SP87-10. CANMET, Ottawa, Ontario, Canada.
10. **Torma, A. E.** 1977. The role of *Thiobacillus ferrooxidans* in hydrometallurgical processes. Adv. Biochem. Eng. **6**:1–37.